
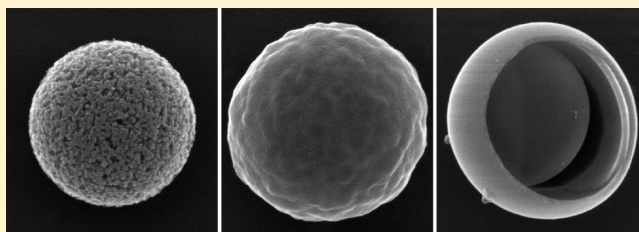


Carbon Microspheres as Supercapacitors

Ho Kim,[†] Maria E. Fortunato,[‡] Hangxun Xu,[‡] Jin Ho Bang,[§] and Kenneth S. Suslick^{*,†,‡}[†]Department of Materials Science and Engineering and [‡]Department of Chemistry, University of Illinois at Urbana–Champaign, 600 South Mathews Avenue, Urbana, Illinois 61801, United States[§]Department of Applied Chemistry, Hanyang University, 55 Hanyangdaehak-ro, Sangnok-gu, Ansan, Kyeonggi-do 426-791, Korea Supporting Information

ABSTRACT: Carbon microstructures fabricated by ultrasonic spray pyrolysis (USP) of aqueous precursors were tested as supercapacitors. USP carbons (USP-C) possess unique physicochemical characteristics, including substantial microporosity and high surface concentrations of oxygenated functional groups. We find that USP-Cs have higher electrochemical double-layer capacitance compared with other carbon structures. Porous carbon microspheres prepared from USP of lithium dichloroacetate, lithium/potassium propiolate, or sucrose produce electrochemical double layer capacitors (EDLCs) that have gravimetric capacitances of 185, 341, and 360 F/g, respectively. Microstructural and chemical analyses of the carbon materials suggest that the observed capacitance is related to the effects of surface functionality.



INTRODUCTION

The increasing energy demands for portable applications (e.g., electronics, power tools, electric vehicles, etc.) have driven the development of alternate energy sources, including lithium-ion secondary batteries, fuel cells, and electrical double-layer capacitors (EDLCs).^{1,2} EDLCs are capable of operating at higher charge/discharge rates, which makes them well-suited for applications that require higher power density. Current commercial EDLCs contain activated carbon materials with specific surface areas (SSAs) of 1000–1500 m²/g and gravimetric capacities of 250 F/g.^{1–6} Because the capacitance limit has been reached with the usual activated carbons, recent research activity has shifted to alternate carbon materials, including carbide thin films,⁷ nanotubes,^{8,9} graphene,^{10–12} polyaniline,^{13,14} or polyaniline/graphene composites.^{15,16} Because of the limited availability and expense of these materials, however, development of new cost-effective and environmentally friendly carbon materials is still needed.

We have previously introduced ultrasonic spray pyrolysis (USP) for the synthesis of microstructured carbon materials and applied them to real applications.^{17–22} For example, USP of a lithium dichloroacetate solution²¹ or a sucrose solution with sodium carbonate²⁰ created microporous carbon microspheres with SSAs of as high as 710 and 698 m²/g, respectively. These SSAs were achieved using environmentally friendly, water-soluble, in situ templates formed during the pyrolysis stage, such as lithium chloride from lithium dichloroacetate or CO₂ and Na₂O from sodium carbonate.

In this work, we report the application of USP carbon microspheres as EDLC electrode materials and the detailed analyses of these materials, which elucidates the importance of

high surface functionality to the creation of these materials' high capacitance.

EXPERIMENTAL SECTION

USP Apparatus. The USP experimental setup (Figure S1 in the Supporting Information) has been described in detail elsewhere.^{20,21} In brief, microdroplets are formed by nebulizing a precursor solution by an ultrasonic nebulizer (1.65 MHz frequency and 5.8 W/cm² of output power). The droplets are suspended in a gas flow and heated by passing through a quartz tube contained in an 800 °C furnace (a total heated region ~30 cm in length), where thermally induced chemical reactions in the droplets or with gaseous reactants convert the precursors to the product powders. The USP carbon syntheses were performed using an inert carrier gas (1.0 standard liter per minute of Ar) to prevent the oxidation of the carbon product.

Materials and Precursor Solution Preparation. Lithium hydroxide (LiOH, 99.5% purity), dichloroacetic acid (Cl₂CH-COOH, 99%), sodium carbonate (Na₂CO₃, 99.5%), propiolic acid (HC≡C-CO₂H, 95%), potassium hydroxide (KOH, 99.5%), and Nafion (perfluorinated ion-exchange resin, 5 wt % solution in a mixture of aliphatic alcohols) were obtained from Sigma-Aldrich, sucrose (C₁₂H₂₂O₁₁, 99%) was obtained from EMD Chemicals, and sulfuric acid (H₂SO₄, 95–98%) was obtained from Mallinckrodt-Baker. USP carbon 1 (USP-C1) was prepared from a lithium dichloroacetate solution, which was

Received: July 26, 2011

Revised: September 9, 2011

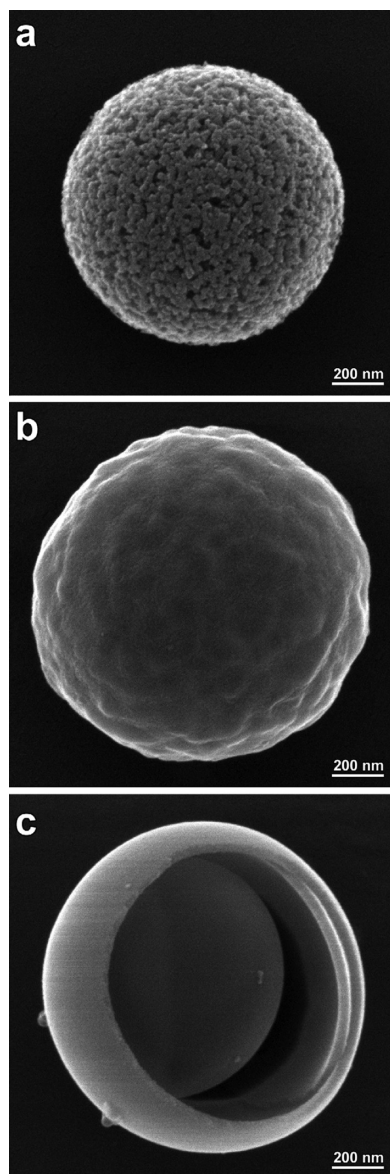


Figure 1. SEM images illustrating the typical morphologies of carbons prepared by ultrasonic spray pyrolysis: (a) USP-C1 from lithium dichloroacetate, (b) USP-C2 from a 1:2 mixture of sucrose and sodium carbonate, and (c) USP-C3 from a 1:3 mixture of potassium propionate and lithium propionate.

prepared by mixing 1.0 M lithium hydroxide solution and 1.0 M dichloroacetic acid solution in 1:1 ratio (v/v). USP carbon 2 (USP-C2) was prepared from a 1:1 ratio (v/v) of 1.0 M sodium carbonate solution and 0.5 M sucrose solution. USP carbon 3 (USP-C3) was prepared from a mixed solution of potassium propionate and lithium propionate in a 1:3 molar ratio in deionized (DI) water; the propionate solutions were separately prepared by from a 1:1 ratio (v/v) of 1 M propiolic acid and 1 M potassium hydroxide and of propiolic acid and lithium hydroxide, respectively.

Product Isolation. As-synthesized particles were collected in DI water-filled bubblers and isolated via centrifugation. The particles were washed three times with DI water to dissolve the salts formed during the USP processes, and the resulting porous carbon materials were isolated by centrifugation (>8000 rpm) and dried in an oven at 90 °C overnight.

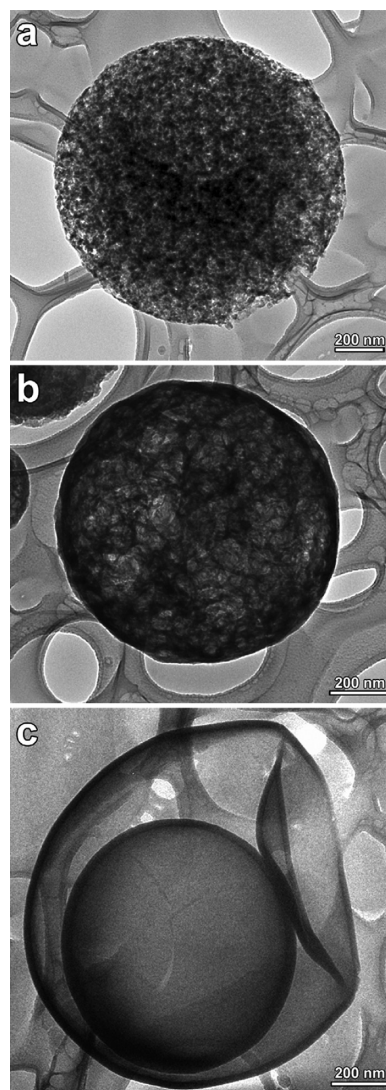


Figure 2. TEM images illustrating the typical morphologies of carbons prepared by ultrasonic spray pyrolysis: (a) USP-C1 from lithium dichloroacetate, with a rough surface; (b) USP-C2 from a 1:2 mixture of sucrose and sodium carbonate, with a smoother microporous surface and porous interior; and (c) USP-C3 from a 1:3 mixture of potassium propionate and lithium propionate, with a smooth microporous shell-in-shell hollow structure.

Characterization of Carbon Powders. Scanning electron micrographs (SEMs) were taken using a JEOL 7000F field-emission (FE)-SEM operating at 15 kV. Transmission electron microscopy (TEM) was conducted using a JEOL 2010F FE-TEM and a JEOL 2010 LaB6 TEM operating at 200 kV to compare carbon inner structures. Surface functionality was analyzed using a PHI 5400 X-ray photoelectron spectroscope (XPS, Physical Electronics, Mg $K\alpha$ source) and a Nicolet Nexus 670 Fourier transform infrared spectroscope (FTIR, Thermo). SSAs and pore size distribution were measured by nitrogen adsorption using a Nova 2200e surface area and pore analyzer (Quantachrome Instruments) at liquid nitrogen temperature (−196 °C) after degassing the samples under vacuum (<0.1 mmHg) at 130 °C overnight.

Capacitance Measurements. Each carbon material was suspended in a Nafion solution (100 μ L of as-received Nafion

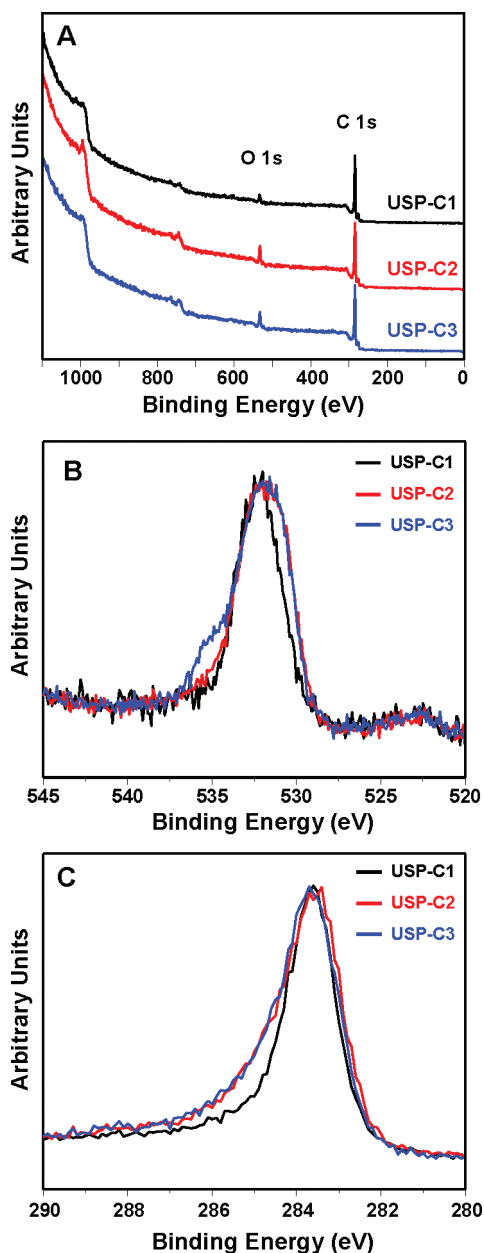


Figure 3. XPS spectra of USP carbon materials. (a) Broad scan (1100–0 eV) spectra normalized to the carbon peaks of the three materials to show the relative intensities of oxygen 1s peaks, (b) O 1s (545–520 eV) spectra, and (c) C 1s (290–280 eV) spectra normalized to the highest peak of each element to show the relative intensities from each functional group type.

mixed with 500 μL of DI water and 500 μL of isopropyl alcohol) and sonicated for at least 1 h to ensure that particles were well-dispersed and wetted with the solution. A carbon film was prepared on a glassy carbon electrode (MF-2012, Bio Analytical Systems, 3.0 mm diameter) by drop-casting the carbon suspension and drying the electrode in a 150 $^{\circ}\text{C}$ oven for 3 min. The electrode was then immersed in a 1.0 M H_2SO_4 solution and electrochemically tested by cyclic voltammetry (CV) in a voltage range of 0 to 0.9 V using a CV-50W voltammetric analyzer (Bio Analytical Systems, Inc.) with a platinum wire counter electrode and a silver/silver chloride (Ag/AgCl) reference electrode. The

measurements for each USP-C were made at five different scan rates (5, 20, 50, 100, and 200 mV/s) to observe the rate dependence of the capacitance.

RESULTS AND DISCUSSION

Morphology of Carbon Microstructures. SEM and TEM analysis show unique morphologies for each USP-C (Figures 1 and 2, Supporting Information Figure S3). USP-C1 (Figures 1A and 2A) possesses an evenly distributed porous carbon network throughout the entire particle, and mesopores are visible on the surface of the particle. Whereas the USP process facilitates spherical particle formation, lithium dichloroacetate melts and decomposes to form LiCl, which acts as an internal sacrificial template as the carbon network growth occurs;²¹ product collection and workup in water removes the salt template and reveals the porous carbon structure. In contrast, USP-C2 has an internal macroporous carbon network and a microporous outer shell (Figures 1B and 2B). This hierarchical porosity is attributed to the gases that are evolved from the decomposition of sucrose and sodium carbonate during the USP-C2 synthesis.²⁰ In the case of USP-C3, a nested sphere-in-sphere morphology is observed (Figures 1C and 2C). The solubility difference between lithium propiolate and potassium propiolate is thought to be responsible for the development of the distinct shell-in-shell morphology. In all three carbon microspheres, the carbon is amorphous and nongraphitic, as shown by high-resolution TEM and by XRD (Figures S4 and S5 in Supporting Information).

The SSAs of USP-C1, USP-C2, and USP-C3 obtained by the three-point BET method were found to be 710, 698, and 565 m^2/g , respectively. Pore size distributions were calculated with the Horvath–Kawazoe model; all USP-Cs have very narrow pore distributions, with the majority of the pores being <1 nm in diameter (Figure S6 in Supporting Information). It is worth noting that pores smaller than 1 nm increase carbon capacitance significantly.²³

Analysis of Surface Functionality. The surface composition of each USP-C was evaluated by XPS (Figure 3). The USP-C surfaces were shown to contain only carbon and oxygen, and the atomic percent composition of each surface was calculated from the XPS data (Table 1). The oxygen peaks of all USP-Cs are not equivalent (Figure 4 and Table 2). There are four types of functional groups that contribute differently to the capacitance: C=O groups at 532 eV, C–OH groups from carboxylic acids at 530.8 eV, C–OH groups attached to aromatic carbons or doubly bonded carbons (Ph–OH or $-\text{C}=\text{C}-\text{OH}$) at 534.9 eV, and ether groups (R–O–R') at 537 eV. On the USP-C1 surface, C=O carbonyl groups are the dominant oxygen functionality (80%). The surface of USP-C2 contains C=O (44%) and C–OH (42%) groups from carboxylic acids, Ph–OH or $-\text{C}=\text{C}-\text{OH}$ groups (10%), and ether functionalities (4%). USP-C3 exhibits the same oxygen functionalities as USP-C2: C=O (39%) and C–OH (40%) groups from carboxylic acids, Ph–OH or $-\text{C}=\text{C}-\text{OH}$ groups (12%), and ether functionalities (9%). The presence of each functional group was confirmed by FTIR (Figure S2 in the Supporting Information).

Capacitance of USP Carbons. The capacitance of the carbon materials (Table 1) was calculated from the CV data (Figure 5). The capacitance calculation was conducted as described in detail elsewhere.²⁴ In brief, gravimetric capacitances (F/g) were calculated by integrating the CV area, divided by the scan rate (mV/s), scan range (0.9 V), and mass of carbon (g) applied.

Table 1. Properties of USP Carbon Materials

precursors	USP-C1	USP-C2	UCPS-3
	lithium dichloroacetate	1:2 mixture of sucrose and sodium carbonate	1:3 mixture of potassium and lithium propionate
specific surface area (m^2/g)	710	698	565
average pore diameter (\AA)	7.1	8.2	7.6
average gravimetric capacitance (F/g)	185 ± 8	360 ± 11	341 ± 13
carbon surface concentration (atomic percent, XPS)	95	88	88
oxygen surface concentration (atomic percent, XPS)	5	12	12

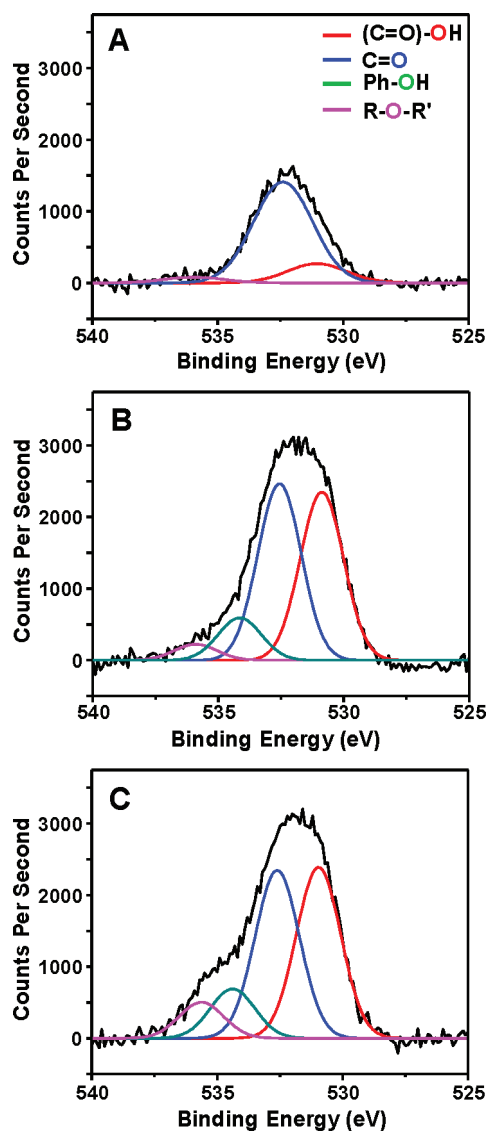


Figure 4. XPS O 1s spectra of (a) USP-C1, (b) USP-C2, and (c) USP-C3 showing deconvolution and fitting with CasaXPS software (version 2.3.12); baseline corrected.

The measurements were repeated for three different batches of each material to show reproducibility. The capacitances (at a scan rate of 5 mV/s) of the USP carbon microspheres were found to be 185 ± 8 F/g for USP-C1, 360 ± 11 F/g for USP-C2, and

Table 2. Composition of Oxygen Functional Groups on USP Carbon Materials (Percent Concentration)

	USP-C1	USP-C2	UCPS-3
$-(\text{C}=\text{O})-\text{OH}$	15	42	39
$>\text{C}=\text{O}$	80	44	40
Ph-OH	0	10	12
R-O-R'	5	4	9

341 ± 13 F/g for USP-C3, whereas the capacitance of commercial DARCO activated carbon (DARCO AC, Sigma-Aldrich, SSA of $886 \text{ m}^2/\text{g}$) was found to be 214 F/g (Figure S7 in the Supporting Information).

Capacitances of USP-Cs do not correlate with the SSAs. For example, USP-C3 has a larger capacitance than USP-C1 (341 and 185 F/g, respectively) but a lower SSA (565 and $710 \text{ m}^2/\text{g}$, respectively). This finding is significantly different from prior reports,^{1,2,5,26} which suggested a linear increase in capacitance with an increase in SSA in carbon materials; the prior studies, however, did not examine materials with significant differences in surface properties or surface functionalities.

The reduced importance of surface area on capacitance and the generally high capacitances of USP-Cs can be rationalized through consideration of their surface functionalities. USP-Cs possess a higher surface concentration of oxygen functional groups compared to other commercially available carbons (Vulcan XC-72R and DARCO AC), which typically have only ~ 2 atomic percent surface oxygen. The influence of oxygen functional groups on the capacitance of carbon materials is well-known from previous literature.^{1,4,27–33} Conway, for example, pointed out that oxygen-related functional groups formed by surface oxidation enhanced capacitance by increased wettability of accessible pores by electrolytes, especially in aqueous solutions, thus helping ions to reach the micropores within carbon materials.¹ In addition to the enhanced wettability, the effect of Faradaic reactions (i.e., electrochemical redox reactions) of the oxygen functional groups have also been reported, which add to the total capacitance as a form of pseudocapacitance.^{4,28,30}

The high concentrations of Ph-OH (or $-\text{C}=\text{C}-\text{OH}$) and R-O-R' groups in USP-C2 and USP-C3 are responsible for their higher capacitances than USP-C1. This is in agreement with previous studies on the effects of selective surface modifications of porous carbon materials.^{27,29,32,34} Carbonyl, Ph-OH (or $-\text{C}=\text{C}-\text{OH}$), or R-O-R' groups increase the capacitance of carbon materials.²⁷ A quantitative relationship between capacitance and the concentrations of each possible surface functionalities, however, has not yet been established. Here our composition

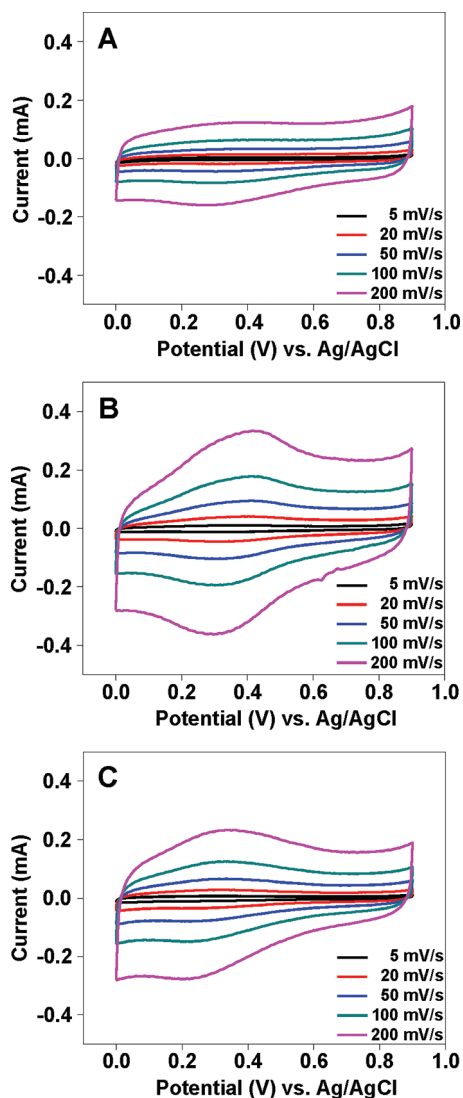


Figure 5. Cyclic voltammograms of USP carbons: (a) USP-C1, (b) USP-C2, and (c) USP-C3 in 1.0 M H_2SO_4 electrolyte solution with an Ag/AgCl reference electrode. Each material was tested at five different scan rates, as indicated.

analysis of oxygen peaks suggests that the advantages of having Ph-OH (or $-\text{C}=\text{C}-\text{OH}$) and R-O-R' groups (14% for USP-C2 and 21% for USP-C3) are substantial.

CONCLUSIONS

We demonstrate in this study that USP-C materials are promising alternatives to commercial active carbon materials for supercapacitor applications. Our USP-Cs were synthesized from water-soluble precursors, which are often less expensive and generally more environmentally friendly than organic precursors. Compared with other synthetic routes, the USP method is superior in introducing various surface functional groups without further oxidation, as usually required for conventional carbon materials. Surface analyses reveal that the observed high capacitance of our USP product is attributed to the combination of sufficiently high surface areas with high concentrations of oxygenated functional groups on the carbon surface. The versatility of USP synthesis can create other carbon materials with

various surface functionalities, which could further enhance applications requiring supercapacitors.

ASSOCIATED CONTENT

S Supporting Information. Schematic of the USP setup and additional characterization of materials are included. This material is available free of charge via the Internet at <http://pubs.acs.org>.

AUTHOR INFORMATION

Corresponding Author

*E-mail: ksuslick@illinois.edu.

ACKNOWLEDGMENT

This research was supported by the U.S. NSF DMR 09-06904. This research was carried out in part in the Center for Microanalysis of Materials, UIUC, which is partially supported by the U.S. Department of Energy under grant DE-FG02-07ER46453 and DE-FG02-07ER46471.

REFERENCES

- (1) Conway, B. E. *Electrochemical Supercapacitors: Scientific Fundamentals and Technological Applications*; Plenum Press: New York, 1999.
- (2) Simon, P.; Gogotsi, Y. *Nat. Mater.* **2008**, *7*, 845–854.
- (3) Frackowiak, E. *Phys. Chem. Chem. Phys.* **2007**, *9*, 1774–1785.
- (4) Kinoshita, K. *Carbon: Electrochemical and Physicochemical Properties*; Wiley: New York, 1988.
- (5) Arico, A. S.; Bruce, P.; Scrosati, B.; Tarascon, J.-M.; van Schalkwijk, W. *Nat. Mater.* **2005**, *4*, 366–377.
- (6) Burke, A. *Electrochim. Acta* **2007**, *53*, 1083–1091.
- (7) Chmiola, J.; Largeot, C.; Taberna, P.-L.; Simon, P.; Gogotsi, Y. *Science* **2010**, *328*, 480–483.
- (8) Kaempgen, M.; Chan, C. K.; Ma, J.; Cui, Y.; Gruner, G. *Nano Lett.* **2009**, *9*, 1872–1876.
- (9) Futaba, D. N.; Hata, K.; Yamada, T.; Hiraoka, T.; Hayamizu, Y.; Kakudate, Y.; Tanaike, O.; Hatori, H.; Yumura, M.; Iijima, S. *Nat. Mater.* **2006**, *5*, 987–994.
- (10) Liu, C.; Yu, Z.; Neff, D.; Zhamu, A.; Jang, B. Z. *Nano Lett.* **2010**, *10*, 4863–4868.
- (11) Yoo, J. J.; Balakrishnan, K.; Huang, J.; Meunier, V.; Sumpter, B. G.; Srivastava, A.; Conway, M.; Mohana Reddy, A. L.; Yu, J.; Vajtai, R.; Ajayan, P. M. *Nano Lett.* **2011**, *11*, 1423–1427.
- (12) Zhu, Y.; Murali, S.; Stoller, M. D.; Ganesh, K. J.; Cai, W.; Ferreira, P. J.; Pirkle, A.; Wallace, R. M.; Cychosz, K. A.; Thommes, M.; Su, D.; Stach, E. A.; Ruoff, R. S. *Science* **2011**, *332*, 1537–1541.
- (13) Lei, Z.; Chen, Z.; Zhao, X. S. *J. Phys. Chem. C* **2010**, *114*, 19867–19874.
- (14) Amarnath, C. A.; Chang, J. H.; Kim, D.; Mane, R. S.; Han, S.-H.; Sohn, D. *Mater. Chem. Phys.* **2009**, *113*, 14–17.
- (15) Wu, Q.; Xu, Y.; Yao, Z.; Liu, A.; Shi, G. *ACS Nano* **2010**, *4*, 1963–1970.
- (16) Zhang, K.; Zhang, L. L.; Zhao, X. S.; Wu, J. *Chem. Mater.* **2010**, *22*, 1392–1401.
- (17) Skrabalak, S. E. *Phys. Chem. Chem. Phys.* **2009**, *11*, 4930–4942.
- (18) Atkinson, J. D.; Fortunato, M. E.; Dastgheib, S. A.; Rostam-Abadi, M.; Rood, M. J.; Suslick, K. S. *Carbon* **2010**, *49*, 587–598.
- (19) Bang, J. H.; Han, K.; Skrabalak, S. E.; Kim, H.; Suslick, K. S. *J. Phys. Chem. C* **2007**, *111*, 10959–10964.
- (20) Fortunato, M. E.; Rostam-Abadi, M.; Suslick, K. S. *Chem. Mater.* **2010**, *22*, 1610–1612.
- (21) Skrabalak, S. E.; Suslick, K. S. *J. Am. Chem. Soc.* **2006**, *128*, 12642–12643.

- (22) Bang, J. H.; Suslick, K. S. *Adv. Mater. (Weinheim, Ger.)* **2010**, *22*, 1039–1059.
- (23) Chmiola, J.; Yushin, G.; Gogotsi, Y.; Portet, C.; Simon, P.; Taberna, P. L. *Science* **2006**, *313*, 1760–1763.
- (24) Niu, J.; Pell, W. G.; Conway, B. E. *J. Power Sources* **2006**, *156*, 725–740.
- (25) Garcia, B. B.; Feaver, A. M.; Zhang, Q.; Champion, R. D.; Cao, G.; Fister, T. T.; Nagle, K. P.; Seidler, G. T. *J. Appl. Phys.* **2008**, *104*, 01430-1–01430-9.
- (26) Panic, V. V.; Stevanovic, R. M.; Jovanovic, V. M.; Dekanski, A. B. *J. Power Sources* **2008**, *181*, 186–192.
- (27) Bleda-Martinez, M. J.; Macia-Agull, J. A.; Lozano-Castell, D.; Morall, E.; Cazorla-Amor, D.; Linares-Solano, A. *Carbon* **2005**, *43*, 2677–2684.
- (28) Frackowiak, E.; Beguin, F. *Carbon* **2001**, *39*, 937–950.
- (29) Hsieh, C.-T.; Teng, H. *Carbon* **2002**, *40*, 667–674.
- (30) Kim, Y.-T.; Ito, Y.; Tadai, K.; Mitani, T.; Kim, U.-S.; Kim, H.-S.; Cho, B.-W. *Appl. Phys. Lett.* **2005**, *87*, 234106-1–234106-3.
- (31) Nian, Y.-R.; Teng, H. *J. Electroanal. Chem.* **2003**, *540*, 119–127.
- (32) Okajima, K.; Ohta, K.; Sudoh, M. *Electrochim. Acta* **2005**, *50*, 2227–2231.
- (33) Ruiz, V.; Blanco, C.; Raymundo-Pinero, E.; Khomenko, V.; Beguin, F.; Santamar, R. *Electrochim. Acta* **2007**, *52*, 4969–4973.
- (34) Kierzek, K.; Frackowiak, E.; Lota, G.; Gryglewicz, G.; Machnikowski, J. *Electrochim. Acta* **2004**, *49*, 515–523.